Journal of Molecular Catalysis A: Chemical xxx (2013) xxx–xxx

Contents lists available at ScienceDirect

Journal of Molecular Catalysis A: Chemical

journal homepage: www.elsevier.com/locate/molcata

Direct conversion of cellulose into acetol on bimetallic Ni-SnO_x/Al_2O_3 catalysts

Tianyin Deng, Haichao Liu*

Beijing National Laboratory for Molecular Sciences, College of Chemistry and Molecular Engineering, Peking University, Beijing 100871, China

ARTICLE INFO

Article history:
Received 17 August 2013
Received in revised form
29 September 2013
Accepted 11 November 2013
Available online xxx

Keywords:
Cellulose
Acetol
Ni catalyst
C—C bond cleavage
Hydrogenation

ABSTRACT

The direct conversion of cellulose into acetol was studied on SnO_x-modified Ni/Al_2O_3 catalysts with different Sn/Ni atomic ratios in the range of 0–2.0. The selectivity to acetol strongly depended on the Sn/Ni ratios, which reached the highest value of 53.9% at the ratio of 0.5, compared at similar cellulose conversions (~20%). On Ni-SnO_x/Al_2O_3 (Sn/Ni = 0.5), cellulose, glucose and fructose converted to acetol in high yields of approximately 35%, 53% and 73%, respectively, at 210 °C and 6 MPa H_2. The effects of the Sn/Ni ratios on the acetol selectivity appear to be related to their effects on the hydrogenation activity of the Ni-SnO_x/Al_2O_3 catalysts that decreased with increase of the Sn/Ni ratios, and to the relative rate between the hydrogenation of C_6 sugar intermediates (e.g. glucose and fructose) and their degradation intermediates (e.g. glyceraldeyde and dihydroxyacetone) involved in the cellulose reaction on the Ni particles and the isomerization of glucose to fructose and their C—C bond cleavage by retro-aldol condensation on the SnO_x domains. Comparison of SnO_x with CeO_x, ZnO_x and AlO_x supported on Al_2O_3 with different basicity suggested that the larger concentration of stronger basic sites on SnO_x facilitated the isomerizaiton of glucose to fructose and its subsequent C—C bond cleavage. These results and their understanding provide guidance for improving the acetol production from cellulose by tuning the catalytic functions required for the involved reactions of hydrogenation on the metal surfaces, and isomerization and C—C bond cleavage on the basic sites.

1. Introduction

Hydrolytic conversion of cellulose to polyols is an important route for cellulose utilization because its structural feature, a linear polysaccharide polymer with multiple hydroxyl groups, makes it a favorable feedstock of polyols [1,2,3a]. Moreover, polyols are promising bio-platform molecules for the efficient production of fuels and value-added chemicals [3b,4]. In this respect, based on the traditional conversion route involving hydrolysis of cellulose to sugars by mineral acids, and subsequent hydrogenation of sugars to hexitols and other polyols on metal-based catalysts [5], numerous efforts have been made to improve the efficiency of the acid and metal catalysts [6,7]. For example, recent studies showed that combination of heteropoly acids and Ru/C catalysts is efficient for cellulose to hexitols [7]. More notably, Fukuoka and Dhepe reported a pioneering approach for the direct conversion of cellulose to hexitols on Pt/Al_2O_3 in the absence of mineral acids [2]. Luo et al. used the H^+ ions reversibly formed from hot water and achieved more efficient hydrolysis of cellulose and formation of hexitols on Ru/C at 245 °C and 6 MPa H_2 [3a]. Combination of such H^+ ions in hot water with different hydrogenation catalysts, such as carbon nanotube supported Ru and H-ZSM-5 supported nickel, leads to significantly improved hexitol yields [8,9].

Hydrolytic hydrogenation of cellulose has also led to the selective synthesis of other polyols, and particularly ethylene glycol and propylene glycol [5,10–12]. Ji et al. reported the first example of the direct conversion of cellulose into ethylene glycol in high yields (~60%) on supported tungsten carbide catalysts (e.g. Ni-W_2C/C) [10a], which can also be achieved by using H_2WO_4 instead with Ru/C [10b]. Recently, Liu et al. found that cellulose can be transformed selectively to sorbitol, 1,2-propanediol and ethylene glycol, strongly depending on the WO_3 domain size, and obtained a ~31% yield of 1,2-propanediol on WO_3/Al_2O_3 (50 wt%) and Ru/C [11a]. Mu and co-workers also reported the direct conversion of cellulose into 1,2-propanediol in a ~34% yield together with a 19% yield of ethylene glycol on Ni/ZnO [12]. It is known that formation of ethylene glycol and propylene glycol involves selective cleavage of C—C bonds of glucose and fructose intermediates, respectively, prior to their hydrogenation to hexitols [11]. These results show the feasibility of the controllable synthesis of polyols by finely tuning the catalytic functions and consequently the relative rates between the hydrogenation of the sugar intermediates and their degradation in the cellulose reaction.

* Corresponding author. Fax: +86 10 6275 4031.
E-mail address: hcliu@pku.edu.cn (H. Liu).

1381-1169/$ – see front matter © 2013 Elsevier B.V. All rights reserved.
http://dx.doi.org/10.1016/j.molcata.2013.11.016

In this work, we report an efficient conversion of cellulose into acetol. Acetol (1-hydroxy-2-propanone) is an important intermediate in the synthesis of acrolein, heterocyclic compounds and pharmaceuticals, or directly used as an additive in food industry, a reducing agent in the textile industry and so on [13–15]. It is currently produced mainly by oxidation of 1,2-propanediol and esterification/alcoholysis of bromide acetone [16]. New processes based on catalytic dehydration of glycerol to acetol have also been explored [17,18]. Recently, we found that SnO_x-modified Pt/Al_2O_3 (Pt-SnO_x/Al_2O_3) catalysts with Sn/Pt atomic ratios above 2 favor the conversion of cellulose to ethylene glycol and especially acetol over hexitols, most likely due to their inferior hydrogenation activity and the reactivity of SnO_x domains for isomerization of glucose to fructose and its subsequent cleavage of the C—C bonds by retro-aldol condensation [19]. We herein extend this preliminary work, and present a systematic study on the selective conversion of cellulose to acetol on Ni-SnO_x/Al_2O_3 bimetallic catalysts with Sn/Ni ratios in the range of 0–2.0. We examine the effect of the hydrogenation activity of Ni-SnO_x/Al_2O_3 on the product distribution, and the mechanism of the SnO_x species active for the selective cleavage of the C—C bonds in glucose and fructose involved in the cellulose conversion on the SnO_x species. Finally, we obtain high acetol yields from cellulose, and also from glucose and fructose, being approximately 35%, 53% and 73%, respectively.

2. Experimental details

2.1. Catalyst preparation

SnO_x-modified Ni/Al_2O_3 (denoted as Ni-SnO_x/Al_2O_3) catalysts with five different Sn/Ni molar ratios in the range of 0–2.0, were prepared by the incipient wetness impregnation of γ-Al_2O_3 (Alfa Aesar, 208 $m^2\,g^{-1}$) with aqueous solutions of $Ni(NO_3)_2{\cdot}6H_2O$ (AR, Beijing Yili Chemical), and of $Ni(NO_3)_2{\cdot}6H_2O$ (AR, Beijing Yili Chemical) and $SnCl_2{\cdot}2H_2O$ (AR, Shantou Xilong Chemical) with several drops of aqueous HCl solution, respectively. The impregnated samples were dried at room temperature for about 12 h and then at 110 °C overnight. Afterwards, they were reduced in a H_2/N_2 (1/4) flow at 600 °C for 4 h. The Ni-SnO_x/Al_2O_3 samples were denoted as Ni-SnO_x(m)/Al_2O_3, where the m in parentheses represents their nominal Sn/Ni atomic ratio. For example, Ni-SnO_x(0.2)/Al_2O_3 represents the sample with a Sn/Ni atomic ratio of 0.2.

SnO_x-modified Pt/Al_2O_3, Ru/Al_2O_3 and Cu/Al_2O_3 catalysts were prepared in the same way using $H_2PtCl_6{\cdot}6H_2O$ (AR, Beijing Chemical), $RuCl_3{\cdot}nH_2O$ (GR, SinopharmChemical) and $Cu(NO_3)_2{\cdot}3H_2O$ (AR, Beijing Yili Chemical), respectively, followed by reduction in a H_2/N_2 (1:4) flow at 400 °C for 4 h. Their nominal metal loadings were 2 wt% Pt, 1 wt% Ru and 5 wt% Cu, respectively, and their Sn/Pt, Sn/Ru or Sn/Cu atomic ratios were 0.5. In a similar way, SnO_x/Al_2O_3 (5 wt% Sn), CeO_x/Al_2O_3 (5.9 wt% Ce), ZnO_x/Al_2O_3 (2.7 wt% Zn) and AlO_x/Al_2O_3 (1.1 wt% Al) with the same metal molar loading were prepared by the incipient wetness impregnation of Al_2O_3 with aqueous solutions of $SnCl_2{\cdot}2H_2O$, $CeCl_3{\cdot}2H_2O$ (AR, SinopharmChemical), $ZnCl_2{\cdot}2H_2O$ (AR, Shantou Xilong Chemical) and $AlCl_3{\cdot}2H_2O$ (AR, SinopharmChemical) with several drops of HCl solution. They were reduced in a H_2/N_2 (1/4) flow at 600 °C for 4 h.

2.2. Catalyst characterization

XRD patterns were recorded on a Rigaku D/MAX-2400 diffractometer using Cu Kα1 radiation (λ = 1.5406 Å) operated at 40 kV and 100 mA. The 2θ angle was scanned in the range of 25–50° at a rate of 4° min^{-1}. TEM images with Energy dispersive X-ray (EDX) analysis were taken on a Philips TEM instrument (Tecnai F30 FEI) operated at 300 kV. Samples were prepared by uniformly dispersing in ethanol and then placing onto carbon-coated copper grids. The average sizes of metal particles and their size distributions were determined by measuring more than 300 particles randomly distributed in the TEM images. Temperature programmed desorption experiments using CO_2 as the probed molecule (CO_2-TPD) were performed on the ChemBET/TPR/TPD unit (Quantachrome). The samples were treated in the cell in a 99.9999% CO_2 flow (30 mL min^{-1}) at 25 °C for 30 min, and then flushed in a He flow for 1 h. Afterwards, the temperature was ramped from 25 °C to 900 °C at 10 °C min^{-1} in a He flow (30 mL min^{-1}). Prior to the measurements, the samples were hydrothermally treated at 210 °C for 1 h, and then dried in a vacuum oven at 25 °C for 12 h.

2.3. Cellulose reaction

Cellulose (microcrystalline, Alfa Aesar) reactions were carried out in a stainless steel autoclave (100 mL) typically at 210 °C and 6 MPa H_2 for 30 min with vigorous stirring at a speed of 800 rpm. In a typical run, 1 g cellulose and 0.4 g catalyst were introduced into the autoclave containing 50 mL H_2O. Afterwards, the reactor was fully purged with H_2 (>99.999%, Beijing Longhui Jingcheng), pressurized with H_2 to 6.0 MPa and then heated to 210 °C which was kept constant during the reaction. After cooling to room temperature in water, the reaction mixture was filtrated and the solids were washed several times with deionized water. The solids including the catalyst and remaining cellulose were washed with acetone three times and then fully dried in an oven at 60 °C for 24 h. Cellulose conversions were determined by the change in the weight of cellulose loaded before and after the reactions. The products in the liquid phase (e.g. polyols) were analyzed by high-performance liquid chromatography (Shimadzu LC-20A) using Bio-Rad Aminex HPX-87H with a RID detector. The product selectivities were reported on a carbon basis.

3. Results and discussion

SnO_x-modified Ni/Al_2O_3 (Ni-SnO_x/Al_2O_3) catalysts with five different Sn/Ni atomic ratios of 0, 0.2, 0.5, 1.0 and 2.0 were examined in the cellulose reaction in water at 210 °C and 6 MPa H_2. As shown in Table 1, the cellulose conversions fell in the range 20–30% after reaction for 0.5 h, but the selectivities to polyols on these catalysts changed significantly with their Sn/Ni ratios. On Ni/Al_2O_3, the hexitol selectivity was 63.3%. The other identified products mainly included pentitols (4.7%), tetritols (2.4%), glycerol (6.1%), 1,2-propanediol (5.2%), lactic acid (1.0%) and ethylene glycol (2.8%) (Table 1 and Table S1). Trace amount of glucose (0.3%) was also detected. The total selectivity to the identified products was 85.8%. The missing carbon balance was most likely due to the formation of the unidentified products (e.g. humins) derived from the condensation or degradation of glucose and other sugar intermediates. Upon addition of a small amount of SnO_x to Ni/Al_2O_3 at a Sn/Ni ratio of 0.2, the hexitol selectivity decreased slightly from 63.3% to 62.6%, and the selectivities to the cracking products (e.g. C_2 and C_3 polyols) remained similar to those on Ni/Al_2O_3. The total selectivity to the identified products reached 88.0%. After the Sn/Ni ratio was increased to 0.5, the hexitol selectivity sharply decreased to as low as 0.2% with the concurrent increase in the acetol selectivity to as high as 53.9%. The selectivities to glycerol and 1,2-propandiol also sharply decreased to 1.5% and nearly zero, respectively. However, further increasing the Sn/Ni ratios to 1.0 and 2.0 led to a slight decrease in the acetol selectivity to 47.1% and 42.9%, and to the concurrent increase in the lactic acid selectivity to 4.9% and 6.0%, respectively. Moreover, the selectivity to the glucose intermediate monotonically increased from 0.5% to 2.8% with increasing the

Please cite this article in press as: T. Deng, H. Liu, J. Mol. Catal. A: Chem. (2013), http://dx.doi.org/10.1016/j.molcata.2013.11.016

Table 1
Cellulose conversion and polyol selectivity on Ni-SnO_x/Al_2O_3 with different Sn/Ni ratios of 0–2.0, and Pt-SnO_x(0.5)/Al_2O_3, Ru-SnO_x(0.5)/Al_2O_3 and Cu-SnO_x(0.5)/Al_2O_3 with a Sn/Ni ratio of 0.5.[a]

Catalyst[b]	Conversion %	Selectivity (%)							
		Glucose	Hexitols[c]	Pentitols and tetritols[d]	Glycerol	1,2-Propanediol	Acetol	Lactic acid	Ethylene glycol
		C_6	C_6	C_5+C_4	C_3	C_3	C_3	C_3	C_2
Ni/Al_2O_3	19.4	0.3	63.3	7.1	6.1	5.2	Trace	1.0	2.8
Ni-SnO_x(0.2)/Al_2O_3	23.2	0.5	62.6	7.6	8.3	5.0	Trace	1.2	2.8
Ni-SnO_x(0.5)/Al_2O_3	22.9	2.3	0.2	4.5	1.5	Trace	53.9	1.5	2.7
Ni-SnO_x(1.0)/Al_2O_3	26.5	2.5	0.0	5.7	1.3	Trace	47.1	4.9	0.9
Ni-SnO_x(2.0)/Al_2O_3	29.8	2.8	0.1	6.0	1.4	Trace	42.9	6.0	1.9
Pt-SnO_x(0.5)/Al_2O_3	24.7	0.3	87.6	8.4	1.7	0.5	Trace	Trace	0.7
Ru-SnO_x(0.5)/Al_2O_3	26.5	4.1	28.8	6.4	6.5	11.5	8.2	1.2	6.5
Cu-SnO_x(0.5)/Al_2O_3	21.7	11.8	0.7	7.8	1.8	0.0	28.0	11.0	1.6
Ni-SnO_x(0.5)/Al_2O_3[e]	93.9	0.3	0.2	2.4	0.8	1.9	37.2	3.2	2.7
Ni-SnO_x(0.5)/Al_2O_3[f]	100	–	3.2	3.5	5.5	3.1	53.0	3.5	5.1
Ni-SnO_x(0.5)/Al_2O_3[g]	100	–	0.2	3.0	2.4	2.0	72.8	6.8	1.4

[a] 1 g cellulose, 0.4 g catalyst, 210 °C, 50 mL H_2O, 6 MPa H_2 and 0.5 h.
[b] Metal loading: 5 wt% Ni, 2 wt% Pt, 1 wt% Ru and 5 wt% Cu.
[c] Sorbitol, mannitol and trace amount of iditol.
[d] Xylitol, arabitol, erythritol and threitol.
[e] Reaction at 240 °C for 0.5 h on Ni-SnO_x(0.5)/Al_2O_3 (2 wt% Ni).
[f] Glucose reaction: 0.2 g glucose, 0.4 g Ni-SnO_x(0.5)/Al_2O_3 (2 wt% Ni), 200 °C, 50 mL H_2O, 6 MPa H_2 and 0.5 h.
[g] Fructose reaction: 0.2 g fructose, 0.4 g Ni-SnO_x(0.5)/Al_2O_3 (2 wt% Ni), 200 °C, 50 mL H_2O, 6 MPa H_2 and 0.5 h.

Sn/Ni ratios in the range 0.2–2.0. Notably, on Ni-SnO_x(0.5)/Al_2O_3, by increasing the cellulose conversion to 93.9% at 240 °C, the selectivity to acetol remained as high as 37.2%, as shown in Table 1, corresponding to approximately 35% yield of acetol. This acetol yield, on the basis of the following discussion and understanding, could be further improved by optimizing the catalyst properties or reaction conditions.

The observed change in the polyol selectivities is consistent with the effect of SnO_x on the hydrogenation activity of these Ni catalysts, which was probed by the hydrogenation of glucose, the key primary intermediate in the cellulose conversion into polyols. As shown in Table 2, Ni/Al_2O_3 showed a 25.8% glucose conversion and 51.7% hexitol selectivity after 10 min at 120 °C and 6 MPa H_2, which decreased to 12.5% and 31.6%, respectively, on Ni-SnO_x(0.2)/Al_2O_3 with a Sn/Ni ratio of 0.2. Fructose was also detected on the two catalysts, as a product from the isomerization of glucose, with a selectivity of 21.3% and 41.7%, respectively (Table 2). By increasing the Sn/Ni ratio from 0.2 to 0.5, the glucose conversion decreased to 8.6%, and only trace amount of hexitols formed. The fructose selectivity accordingly increased to 71.1%, which further increased to 94.2% at a 6.0% conversion on Ni-SnO_x(2.0)/Al_2O_3 with a Sn/Ni ratio of 2.0. Clearly, the Ni-SnO_x/Al_2O_3 catalysts with the Sn/Ni ratios of 0.5–2.0 exhibited inferior hydrogenation activities, and favored the isomerization of glucose to fructose, which thus renders it possible, under the cellulose reaction conditions in this work, to degrade to C_3 intermediates (e.g. pyruvaldehyde) and ultimately to form the C_3 products including acetol [20–22], as indeed observed at the Sn/Ni ratios exceeding 0.2 (Table 1). Taken together, the observed volcano-shaped change of the acetol selectivity with the Sn/Ni ratios, and its highest value obtained at the ratio of 0.5 (Table 1) suggest that the favorable formation of acetol in the cellulose reaction requires an appropriate hydrogenation activity of the Ni-SnO_x/Al_2O_3 catalysts to meet the requirements for the involved reactions including the hydrogenation of glucose, fructose and C_3 (e.g. glyceraldehyde and dihydroxyacetone) intermediates on the Ni surfaces and their degradation on the basic SnO_x species, as discussed below.

To understand such SnO_x effects on the hydrogenation activity of the Ni-SnO_x/Al_2O_3 catalysts, they were characterized by XRD, TEM and EDX (Figs. 1 and 2 and Fig. S1). Fig. 1 shows the XRD patterns of

Table 2
Glucose hydrogenation on Ni-SnO_x/Al_2O_3 with different Sn/Ni ratios of 0–2.0, Pt-SnO_x(0.5)/Al_2O_3, Ru-SnO_x(0.5)/Al_2O_3 and Cu-SnO_x(0.5)/Al_2O_3 catalysts.[a]

Catalyst[b]	Conversion%	Selectivity (%)	
		Hexitols	Fructose
Ni/Al_2O_3	25.8	51.7	21.3
Ni-SnO_x(0.2)/Al_2O_3	12.5	31.6	43.7
Ni-SnO_x(0.5)/Al_2O_3	8.6	Trace	71.1
Ni-SnO_x(1.0)/Al_2O_3	8.7	Trace	79.1
Ni-SnO_x(2.0)/Al_2O_3	6.0	Trace	94.2
Pt-SnO_x(0.5)/Al_2O_3	61.1	91.0	Trace
Ru-SnO_x(0.5)/Al_2O_3	19.5	82.2	12.5
Cu-SnO_x(0.5)/Al_2O_3	12.4	Trace	53.4
None	0.5	–	–

[a] 1 g glucose, 0.4 g catalyst, 120 °C, 50 mL H_2O, 6 MPa H_2, 10 min.
[b] Metal loading: 5 wt% Ni, 2 wt% Pt, 1 wt% Ru and 5 wt% Cu.

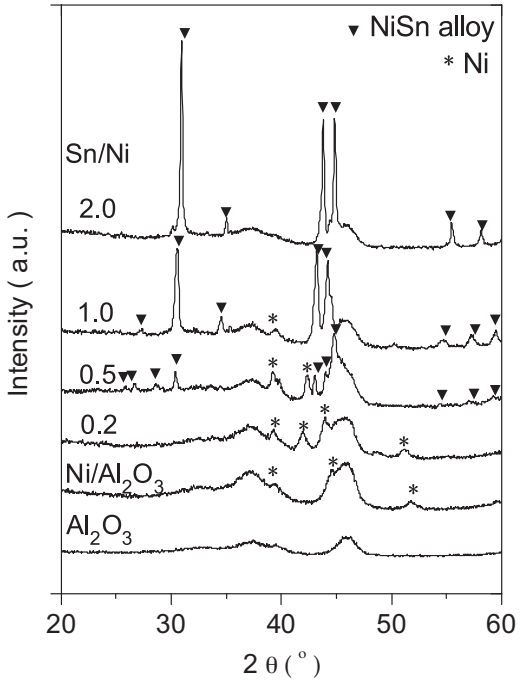

Fig. 1. XRD patterns of Ni-SnO_x/Al_2O_3 (~5 wt% Ni) with different Sn/Ni atomic ratios in the range of 0–2.0.

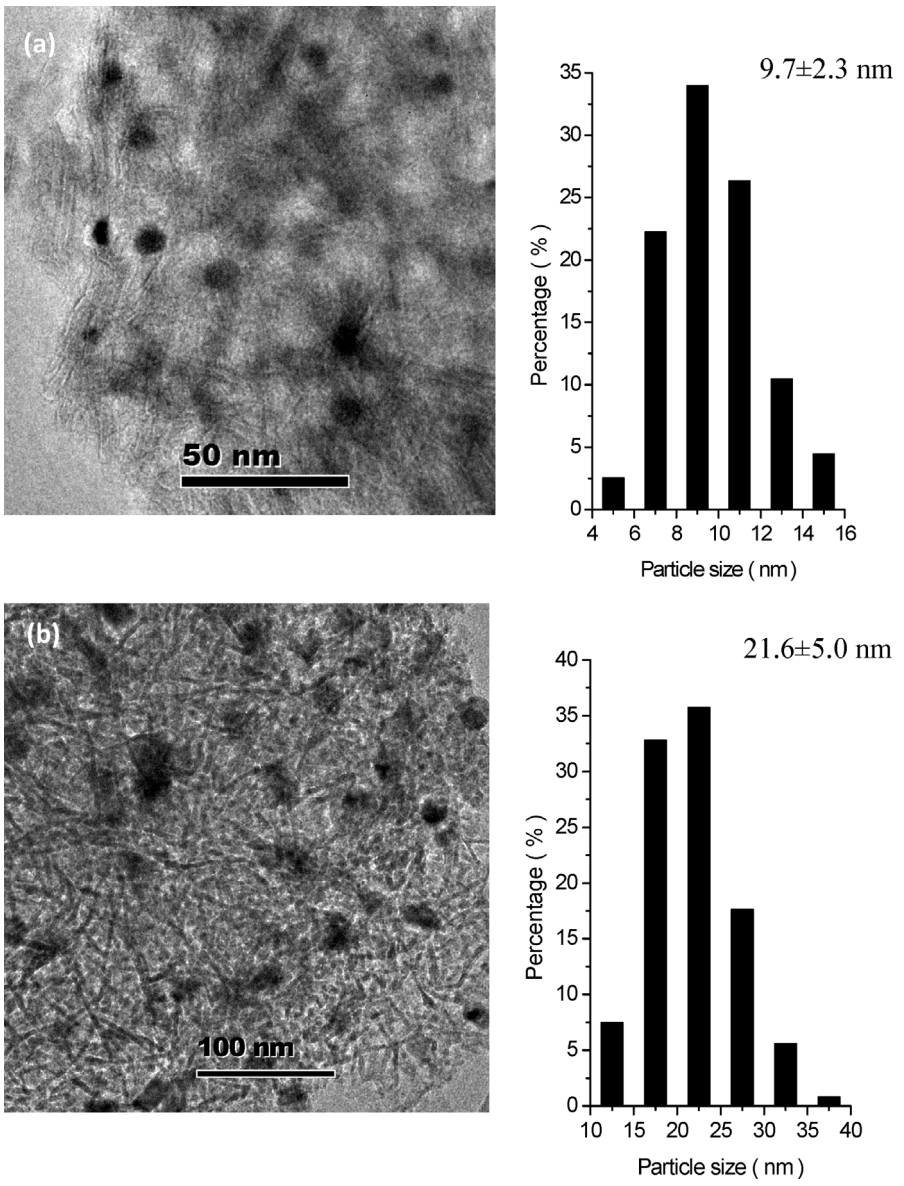

Fig. 2. TEM images and histograms of Ni particle size distribution for Ni/Al_2O_3 (a) and $Ni\text{-}SnO_x(0.2)/Al_2O_3$ (b) (~5 wt% Ni loading).

the Ni/Al_2O_3 and $Ni\text{-}SnO_x/Al_2O_3$ samples. For comparison, the pattern of Al_2O_3 is also included. The Ni crystalline diffraction peaks at 44.4° and 51.8° (JCPDS: 65-2865) were observed on Ni/Al_2O_3, and their intensity increased on $Ni\text{-}SnO_x(0.2)/Al_2O_3$, indicating the formation of larger Ni particles on $Ni\text{-}SnO_x(0.2)/Al_2O_3$. This result is consistent with their TEM images (Fig. 2), showing that the Ni particles possessed mean diameters of 9.7 nm and 21.6 nm, respectively, on Ni/Al_2O_3 and $Ni\text{-}SnO_x(0.2)/Al_2O_3$. New diffraction peaks appeared at 30.5°, 34.6°, 43.2°, 44.2°, 55.0°, 57.2°, and 59.5° when the Sn/Ni ratios exceeded 0.5, which increased in intensity with increasing the Sn/Ni ratios (Fig. 1). These peaks are tentatively assigned to the Ni_3Sn_2 alloy (JCPDS: 65-1315) [23]. However, these diffraction peaks shifted slightly to higher 2θ values (i.e. 30.9°, 35.0°, 43.8°, 44.8°, 55.5°, 58.1°, and 60.1°) at the Sn/Ni ratio of 2.0, most likely due to the formation of Ni_3Sn_4 alloy (JCPDS: 04-0845). The formation of the Ni-Sn alloys on these catalysts with the Sn/Ni ratios higher than 0.5 was confirmed by the representative EDX result for $Ni\text{-}SnO_x(0.5)/Al_2O_3$ (Sn/Ni = 0.5), showing a parallel variation of the relative Ni and Sn compositions against the line-scan positions (Fig. S1). It has been reported that the hydrogenation activities of different Ni species are in the sequence $Ni > Ni_3Sn > Ni_3Sn_2 \gg Ni_3Sn_4$ [23]. These characterization results may account for the observed lower hydrogenation activities for the $Ni\text{-}SnO_x/Al_2O_3$ catalysts with the higher Sn/Ni ratios.

The observed effects of the hydrogenation activity on the polyol selectivities in the cellulose reaction were further confirmed by the results with the SnO_x modified Pt/Al_2O_3, Ru/Al_2O_3 and Cu/Al_2O_3 catalysts (at a Sn/metal atomic ratio of 0.5). As probed by the glucose reaction (Table 2), $Pt\text{-}SnO_x(0.5)/Al_2O_3$ was very active and selective for the glucose hydrogenation to hexitols, affording a 61.1% conversion and 91.0% selectivity after 10 min at 120 °C and 6 MPa H_2, which decreased to 19.5% and 82.2%, respectively, on $Ru\text{-}SnO_x(0.5)/Al_2O_3$ with the concurrent formation of fructose with a 12.5% selectivity. $Cu\text{-}SnO_x(0.5)/Al_2O_3$, resembling the aforementioned $Ni\text{-}SnO_x(0.5)/Al_2O_3$, catalyzed the glucose reaction mainly to fructose with a 53.4% selectivity at a 12.4% glucose conversion. Such different hydrogenation activities of the four SnO_x-modified catalysts led to their different product distributions in the cellulose reaction, as observed on $Ni\text{-}SnO_x/Al_2O_3$ with the different Sn/Ni ratios. As shown in Table 1, due to

its superior hydrogenation activity, cellulose converted to hexitols with a selectivity of as high as 87.6% on Pt-SnO_x(0.5)/Al_2O_3, similar to the result reported previously [19]. The hexitol selectivity declined to 28.8% on Ru-SnO_x(0.5)/Al_2O_3, and to nearly zero (<1%) on Cu-SnO_x(0.5)/Al_2O_3 and Ni-SnO_x(0.5)/Al_2O_3 at the similar cellulose conversions (19.4–26.5%). In contrast, the combined selectivity to the identified C_2 and C_3 products increased from 2.9% on Pt-SnO_x(0.5)/Al_2O_3 to 32.2%, 31.4% and 58.1%, respectively, on Ru-SnO_x(0.5)/Al_2O_3, Cu-SnO_x(0.5)/Al_2O_3 and Ni-SnO_x(0.5)/Al_2O_3. Specifically, the acetol selectivity increased from nearly zero on Pt-SnO_x(0.5)/Al_2O_3 to 8.2% on Ru-SnO_x(0.5)/Al_2O_3, and then further to 28.0% on Cu-SnOx(0.5)/Al_2O_3 and 53.9% on Ni-SnO_x(0.5)/Al_2O_3. The lactic acid selectivity was conversely higher on Cu-SnO_x(0.5)/Al_2O_3 than on Ni-SnO_x(0.5)/Al_2O_3 (11.0% vs. 1.5%). It is known that acetol and lactic acid are formed competitively from the same intermediate, i.e. pyruvaldehyde, via hydrogenation on metal surfaces and benzilic acid rearrangement with bases, respectively [19,22]. Therefore, relative to Ni-SnO_x(0.5)/Al_2O_3, such lower acetol selectivity and higher lactic acid selectivity of Cu-SnO_x(0.5)/Al_2O_3 indicates its inferior hydrogenation activity, together with its higher selectivity to glucose (11.8% vs. 2.3%). Clearly, Ni-SnO_x(0.5)/Al_2O_3 is superior to the other metal-based catalysts in term of the formation of the C_3 products including particularly acetol. The observed SnO_x effects reflects the bifunctional catalysis in the formation of the C_3 products, as discussed previously in the literature [19], and their selectivity relies on the relative rates of the competitive reactions catalyzed by the metal surfaces and basic sites, respectively. Next, we further examine the effects of such bifunctions of the Ni-SnO_x/Al_2O_3 catalysts on the cellulose reaction.

Recently, we reported the cellulose conversion to the C_2 and C_3 products on Pt-SnO_x/Al_2O_3 in the presence of segregated SnO_x species, in which SnO_x is proposed as a base to catalyze the isomerization of glucose to fructose and their retro-aldol condensation [19]. To further understand such function of the SnO_x species in breaking the C—C bonds, three other metal oxides supported on Al_2O_3, CeO_x/Al_2O_3, ZnO_x/Al_2O_3 and AlO_x/Al_2O_3, physically mixed with Ni/Al_2O_3, were compared with SnO_x/Al_2O_3 in the cellulose reaction. Their basicity was probed by CO_2-TPD. As shown in Fig. 3, three or four CO_2 desorption peaks, corresponding to different strength of basic sites, were observed in the range 100–800 °C on these Al_2O_3-supported oxides. The low-temperature peak around 200 °C was assigned to the desorption of the bidentate carbonate species on weaker basic sites, and the peaks above 300 °C were related to the unidentate species desorbed from stronger basic sites [24–26]. Accordingly, the concentrations of their basic sites, based on their CO_2 uptakes, were estimated and listed in Table 3. The total concentrations of the basic sites were 13.2 μmol/g and 11.7 μmol/g for ZnO_x/Al_2O_3 and AlO_x/Al_2O_3, respectively, lower than the value (21.2 μmol/g) for pure Al_2O_3 support, which increased to 40.5 μmol/g and 69.3 μmol/g for SnO_x/Al_2O_3 and CeO_x/Al_2O_3. Among them, SnO_x/Al_2O_3 possessed

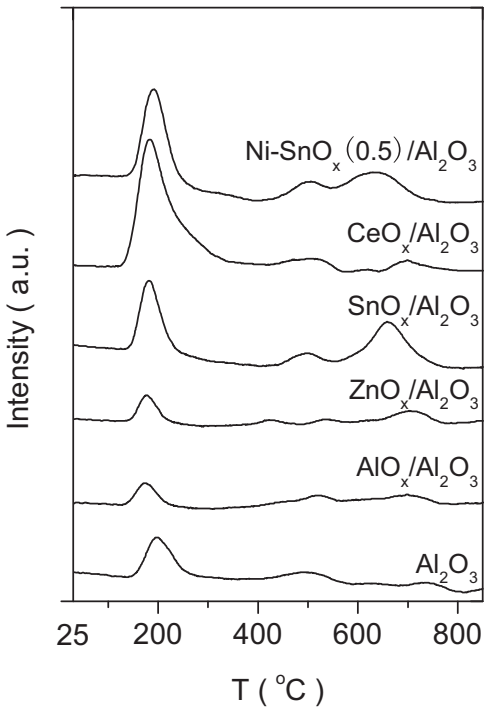

Fig. 3. CO_2-TPD profiles of SnO_x/Al_2O_3, CeO_x/Al_2O_3, ZnO_x/Al_2O_3 and AlO_x/Al_2O_3.

Table 3
The concentrations of basic sites with different strength on Al_2O_3-supported SnO_x, CeO_x, ZnO_x, and AlO_x samples, and Ni-SnO_x(0.5)/Al_2O_3.

Sample	Concentration of basic sites (μmol/g)		
	Weak	Strong	Total
AlO_x/Al_2O_3	6.1	5.6	11.7
ZnO_x/Al_2O_3	6.3	6.9	13.2
CeO_x/Al_2O_3	60.9	8.4	69.3
SnO_x/Al_2O_3	19.1	21.4	40.5
Al_2O_3	14.9	6.3	21.2
Ni-SnO_x(0.5)/Al_2O_3	32.1	25.5	57.6

the largest amount of strong basic sites (~21.4 μmol/g), similar to the value for the Ni-SnO_x(0.5)/Al_2O_3 catalyst. Such different basicity of these supported oxides led to the different cellulose conversion and product distribution. As shown in Table 4, the cellulose conversions varied in the range of 16.1–28.0%, most likely due to the expected effect of the basicity of the supported oxides on the concentrations of H^+ ions generated from hot water under the reaction conditions employed here. Addition of ZnO_x/Al_2O_3 and AlO_x/Al_2O_3 with Ni/Al_2O_3 led to the increase in the selectivtity to the detected C_2 and C_3 products (including glycerol, 1,2-propanediol, acetol, lactic acid and ethylene glycol) from 15.1% to 29.1% and 39.2%,

Table 4
Cellulose conversion and polyol selectivity on four different Al_2O_3 supported oxides physically mixed with Ni/Al_2O_3.[a]

Catalyst	Conversion %	Selectivity (%)							
		Glucose	Hexitols[b]	Pentitols and tetritols[c]	Glycerol	1,2-Propanediol	Acetol	Lactic acid	Ethylene glycol
		C_6	C_6	C_5+C_4	C_3	C_3	C_3	C_3	C_2
Ni/Al_2O_3 + SnO_x/Al_2O_3	16.1	2.6	12.3	6.0	4.8	28.6	16.4	1.5	26.9
Ni/Al_2O_3 + CeO_x/Al_2O_3	19.0	Trace	11.0	6.9	5.4	23.3	Trace	5.6	28.1
Ni/Al_2O_3 + ZnO_x/Al_2O_3	28.0	1.2	41.7	6.0	9.6	12.7	Trace	1.4	5.5
Ni/Al_2O_3 + AlO_x/Al_2O_3	27.6	0.7	46.4	7.3	11.1	13.6	2.3	1.1	6.0

[a] 1 g cellulose, 0.3 g Ni/Al_2O_3 (5 wt%), 0.4 g SnO_x/Al_2O_3 (or CeO_x/Al_2O_3, ZnO_x/Al_2O_3, AlO_x/Al_2O_3), 210 °C, 50 mL H_2O, 6 MPa H_2, 1 h.
[b] Sorbitol, mannitol and trace amount of iditol.
[c] Xylitol, arabitol, erythritol and threitol.

Please cite this article in press as: T. Deng, H. Liu, J. Mol. Catal. A: Chem. (2013), http://dx.doi.org/10.1016/j.molcata.2013.11.016

respectively, which further increased to 62.4% and 78.2% when more basic CeO_x/Al_2O_3 and SnO_x/Al_2O_3 were present instead. Conversely, the selectivity to hexitols decreased from 63.3% to 41.7% and 46.4% in the presence of ZnO_x/Al_2O_3 and AlO_x/Al_2O_3, respectively. The hexitol selectivity further decreased to only 12.3% and 11.0% on SnO_x/Al_2O_3 and CeO_x/Al_2O_3, respectively. Such close correlation between the product selectivities and the basicity of the supported oxides confirms the role of the basic sites in the cleavage of the C—C bonds and the formation of the C_2 and C_3 products.

Further experiments showed that in the presence of given amount of SnO_x/Al_2O_3, the formation of the C_2 and C_3 products also strongly depended on the hydrogenation activity of the Ni/Al_2O_3 catalyst, which was changed by varying its amount in its physical mixture with SnO_x/Al_2O_3. As shown in Fig. 4, with increasing the amount of Ni/Al_2O_3 from 0.1 g to 0.4 g in the presence of 0.4 g SnO_x/Al_2O_3, the selectivities to hexitols, as expected, increased monotonically from 4.5% to 18.7% at similar cellulose conversions (~20%). However, the total selectivities to the C_3 polyols (including glycerol, 1,2-propanediol and acetol) increased from 39.9% to 49.8% with increasing the Ni/Al_2O_3 amount from 0.1 g to 0.3 g, and then decreased to 44.8% when 0.4 g of Ni/Al_2O_3 was present. Similar to this trend, the selectivities to these C_3 and C_2 polyols (i.e. ethylene glycol) reached the maximum value of 76.8% at 0.3 g of Ni/Al_2O_3. The total selectivities to lactic acid and glycolic acid decreased from 5.0% to 1.2% with increasing the Ni/Al_2O_3 amount in the range of 0.1–0.4 g.

Furthermore, the C_3 products were noted to be always dominant over the C_2 products on these SnO_x-containing physical mixtures and SnO_x-modified Ni/Al_2O_3 catalysts, as shown in Fig. 4

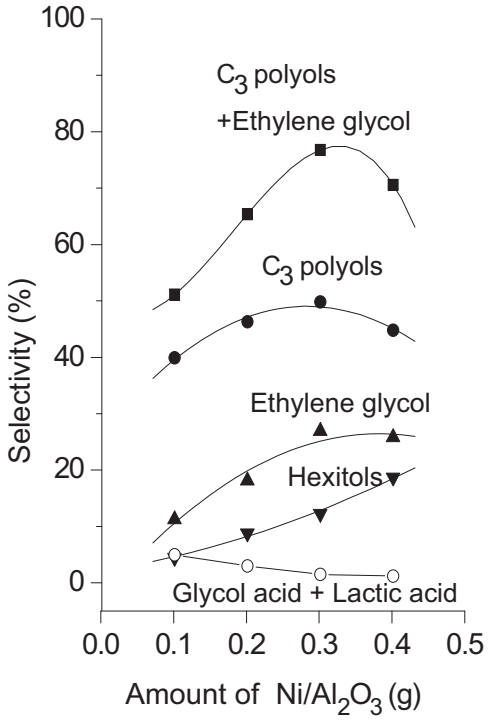

Fig. 4. Cellulose conversions and polyol selectivities as a function of the amount of Ni/Al_2O_3 physically mixed with SnO_x/Al_2O_3 (1 g cellulose, 0.4 g SnO_x/Al_2O_3 with 5 wt% Sn, 50 mL H_2O, 6 MPa H_2, 210 °C, 0.5 h).

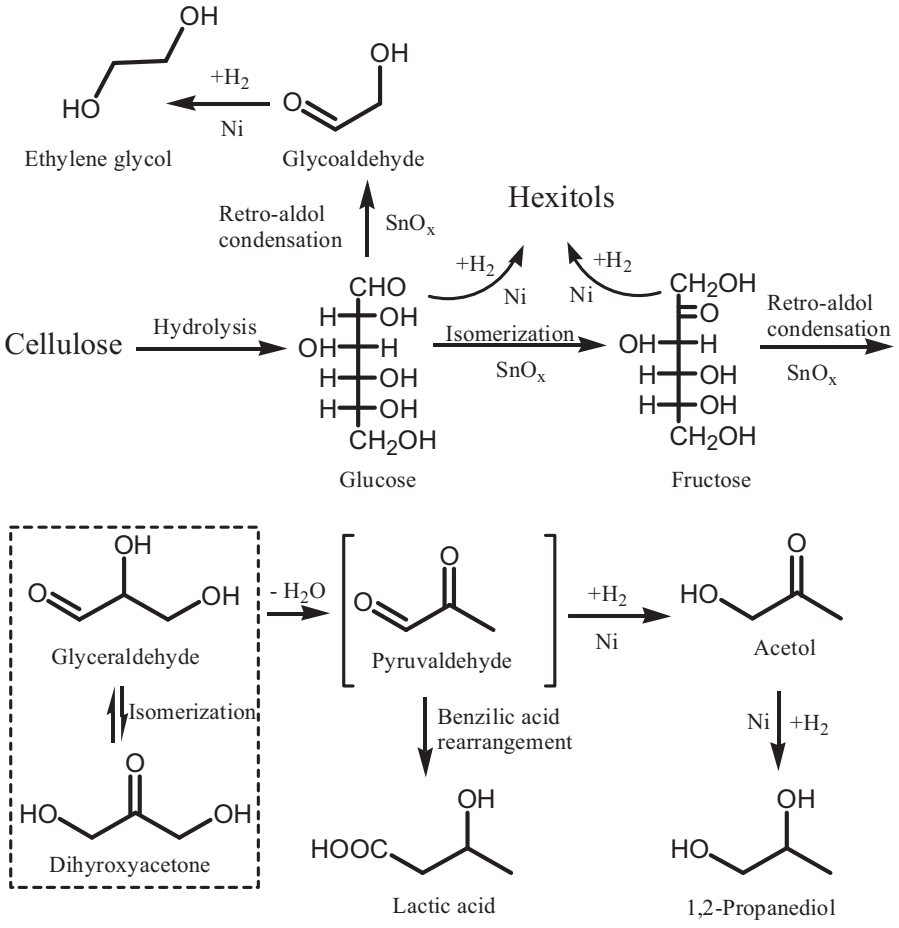

Scheme 1. Plausible cellulose reaction pathways on Ni-SnO_x/Al_2O_3 catalysts.

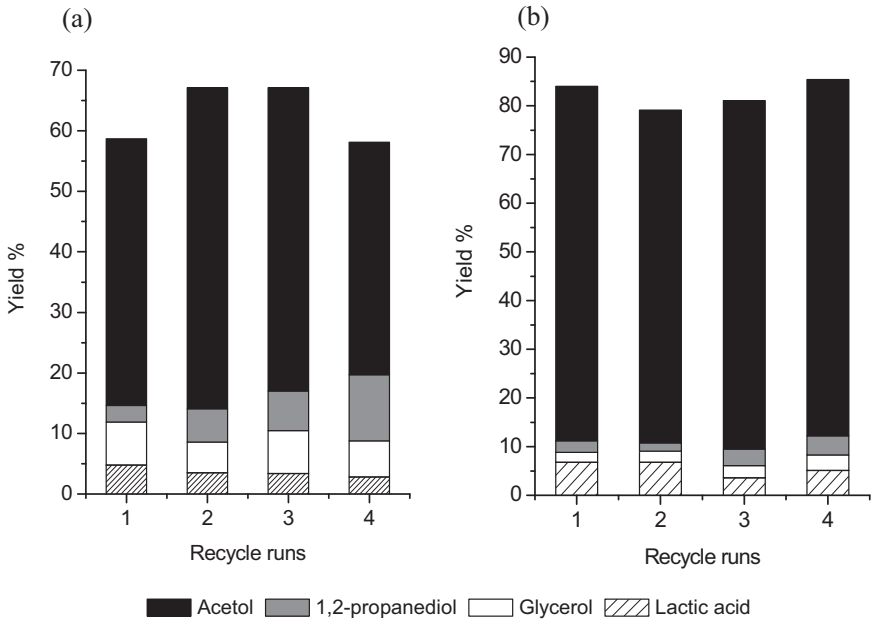

Fig. 5. Yields of C_3 products (acetol, glycerol, 1,2-propanediol and lactic acid) for the four successive reaction cycles of glucose (a) and fructose (b) reaction on Ni-SnO_x(0.5)/Al_2O_3 (0.2 g glucose or fructose, 0.4 g Ni-SnO_x(0.5)/Al_2O_3 catalyst, 50 mL H_2O, 200 °C, 6.0 MPa H_2, 0.5 h).

and Tables 1 and 3. Following the retro-aldol condensation mechanism, glucose tends to form the C_2 products while the C_3 products dominate in the fructose reaction. Therefore, it appears that the predominant formation of the C_3 products including acetol in the cellulose reaction on Ni-SnO_x/Al_2O_3, as depicted in Scheme 1, involves the efficient isomerization of glucose to fructose on SnO_x, following the cellulose hydrolysis to glucose in hot water and before it undergoes hydrogenation to hexitols on the Ni surfaces and retro-aldol condensation to the glycoaldehyde intermediate on the SnO_x species, which is consistent with the observed conversion of glucose to fructose on the Ni-SnO_x/Al_2O_3 catalysts at 120 °C (Table 2). Fructose degrades by retro-aldol condensation on SnO_x to form the glyceraldehyde and dihydroxyacetone intermediates, which undergo hydrogenation to glycerol and further to 1,2-propanediol [20], or dehydration to pyruvaldehyde [21]. The pyruvaldehyde intermediate then converts competitively to acetol and lactic acid via hydrogenation on Ni and benzilic acid rearrangement with SnO_x, respectively [22]. The glycoaldehyde intermediate is ultimately hydrogenated to ethylene glycerol on Ni.

Such proposed reaction pathways are further confirmed by the separate reactions of glucose and fructose on Ni-SnO_x(0.5)/Al_2O_3, leading to the predominant formation of the C_3 products, acetol, 1,2-propanediol, glycerol and lactic acid. As shown in Table 1, after 30 min at 200 °C and 6 MPa H_2, the glucose and fructose conversions reached 100%, and the yields to the C_3 products were 65.1% and 84.0%, respectively, in which the acetol yields were 53.0% and 72.8%. Together with the aforementioned acetol yield (34.9%) in the cellulose reaction, these are the highest acetol yields that have been reported to date directly from cellulose and its derivatives. These high acetol yields on Ni-SnO_x(0.5)/Al_2O_3, together with its stability and recyclability, as discussed below, demonstrate the potential property of the Ni-SnO_x/Al_2O_3 catalysts for the direct transformation of cellulose and its derivatives (e.g. glucose and fructose) to acetol.

The stability and recyclability of the Ni-SnO_x/Al_2O_3 catalysts were examined, and Fig. 5 shows the representative results on Ni-SnO_x(0.5)/Al_2O_3 in the reactions of glucose and fructose at 200 °C and 6 MPa H_2. No significant decline in the yields of the C_3 products (i.e. acetol, 1,2-propanediol, glycerol and lactic acid) was observed after recycling the Ni-SnO_x(0.5)/Al_2O_3 catalyst over four times. This is consistent with the XRD characterization result for this catalyst, showing essentially identical XRD patterns (Fig. S2) before and after the four cycles. However, pure Al_2O_3 support readily transformed into hydrated boehmite (AlOOH) phase in water at 200 °C, as shown in Fig. S2. These results show the enhanced hydrothermal stability of Al_2O_3 by loading SnO_x on its surface, as also found with the Pt-SnO_x/Al_2O_3 and WO_x/Al_2O_3 catalysts [11a,19], which is most likely achieved via the efficient blocking of the surface hydroxyl groups by SnO_x on Al_2O_3 to inhibit its hydration and the boehmite formation, as proposed by Ravenelle et al. [27].

4. Conclusions

Cellulose conversion to polyols on Ni-SnO_x/Al_2O_3 catalysts strongly depends on their Sn/Ni atomic ratios in the range of 0–2.0, as a result of their lower hydrogenation activity at the higher Sn/Ni ratios. Compared at similar cellulose conversions, the Ni-SnO_x/Al_2O_3 catalyst at the Sn/Ni ratio of 0.5 exhibits the highest acetol selectivity, reflecting the requirements of the catalytic functions for the cellulose conversion to acetol involving the isomerization of glucose to fructose, the cleavage of the C—C bonds of fructose to form the pyruvaldehyde intermediate on the basic SnO_x domains, and the subsequent pyruvaldehyde hydrogenation on the Ni particles. Compared to CeO_x, ZnO_x and AlO_x supported on Al_2O_3 with different basicity, it appears that the larger concentration of stronger basic sites on SnO_x may contribute to its superior performance for the isomerizaiton of glucose to fructose and C—C bond cleavage. On Ni-SnO_x/Al_2O_3 (Sn/Ni = 0.5), reactions of cellulose, glucose and fructose afford high acetol yields of 34.9%, 53.0% and 72.8%, respectively, at 210 °C and 6 MPa H_2. Such high yields, based on the findings in this work, can be further improved by optimizing the catalytic functions required for the involved reactions of hydrogenation, isomerization and C—C bond cleavage.

Acknowledgements

This work was supported by the National Natural Science Foundation of China (21173008, 21373019 and 51121091) and

the National Basic Research Project of China (2011CB808700 and 2011CB201400).

Appendix A. Supplementary data

Supplementary data associated with this article can be found, in the online version, at http://dx.doi.org/10.1016/j.molcata.2013.11.016.

References

[1] J.A. Geboers, S. Van de Vyver, R. Ooms, B. Op de Beeck, P.A. Jacobs, B.F. Sels, Catal. Sci. Technol. 1 (2011) 714–726.
[2] A. Fukuoka, P.L. Dhepe, Angew. Chem. Int. Ed. 45 (2006) 5161–5163.
[3] (a) C. Luo, S. Wang, H.C. Liu, Angew. Chem. Int. Ed. 46 (2007) 7636–7639;
(b) Y. Shen, S. Wang, C. Luo, H.C. Liu, Prog. Chem. 19 (2007) 431–436.
[4] A. Corma, S. Iborra, A. Velty, Chem. Rev. 107 (2007) 2411–2502.
[5] (a) J.M. Robinson, C.E. Bungess, M.A. Bently, C.D. Brasher, B.O. Horre, D.M. Lillard, J.M. Macias, H.D. Mandal, S.C. Mills, K.D.O. Harra, J.T. Pon, A.F. Raigoza, E.H. Sanchez, J.S. Villarreal, Biomass Bioenergy 26 (2004) 473–483;
(b) V.I. Sharkov, Angew. Chem. Int. Ed. Engl. 2 (1963) 405–409;
(c) N. Yan, C. Zhao, C. Luo, P.J. Dyson, H.C. Liu, Y. Kou, J. Am. Chem. Soc. 128 (2006) 8714–8715.
[6] (a) R. Palkovits, K. Tajvidi, A.M. Ruppert, J. Procelewska, Chem. Commun. 47 (2010) 576–578;
(b) R. Palkovits, K. Tajvidi, J. Procelewska, R. Rinaldi, A. Ruppert, Green Chem. 12 (2010) 972–978.
[7] (a) J. Geboers, S. Van de Vyver, K. Carpentier, K. de Blochouse, P. Jacobs, B. Sels, Chem. Commun. 46 (2010) 3577–3579;
(b) J. Geboers, S. Van de Vyver, K. Carpentier, P. Jacobs, B. Sels, Chem. Commun. 47 (2011) 5590–5592.
[8] W. Deng, X. Tan, W. Fang, Q. Zhang, Y. Wang, Catal. Lett. 133 (2009) 167–174.
[9] G. Liang, H. Cheng, W. Li, L. He, Y. Yu, F. Zhao, Green Chem. 14 (2012) 2146–2149.
[10] (a) N. Ji, T. Zhang, M. Zheng, A. Wang, H. Wang, X. Wang, J.G.G. Chen, Angew. Chem. Int. Ed. 47 (2008) 8510–8513;
(b) Z. Tai, J. Zhang, A. Wang, M. Zheng, T. Zhang, Chem. Commun. 48 (2012) 7052–7054.
[11] (a) Y. Liu, C. Luo, H. Liu, Angew. Chem. Int. Ed. 51 (2012) 3249–3253;
(b) T. Deng, J. Sun, H. Liu, Sci. China Chem. 53 (2010) 1476–1480.
[12] X. Wang, L. Meng, F. Wu, Y. Jiang, L. Wang, X. Mu, Green Chem. 14 (2012) 758–765.
[13] S. Sato, D. Sakai, F. Sato, Y. Yamada, Chem. Lett. 41 (2012) 965–966.
[14] D. Stoštić, S. Bennici, S. Sirotin, C. Calais, J.L. Couturier, J.L. Dubois, A. Travert, A. Auroux, Appl. Catal. A 447–448 (2012) 124–134.
[15] M.H. Mohamad, R. Awang, W.M.Z.W. Yunus, Am. J. Appl. Sci. 8 (2011) 1135–1139.
[16] N. Li, Y. Ji, B. Zeng, W. Shen, H. Xu, Chem. World 7 (2009) 421–423, 448.
[17] F. Theo, G. Gerd, H. Klaus, DE4128692A1.
[18] (a) S. Sato, M. Akiyama, R. Takahashi, T. Hara, K. Inui, et al., Appl. Catal. 347 (2008) 186–191;
(b) W. Suprun, M. Lutecki, T. Haber, H. Papp, J. Mol. Catal. A 309 (2009) 71–78;
(c) A.K. Kinage, P.P. Upare, P. Kasinathan, Y.K. Hwang, J.S. Chang, Catal. Commun. 11 (2010) 620–623;
(d) A. Yamaguchi, N. Hiyoshi, O. Sato, M. Shirai, Top. Catal. 53 (2010) 487–491.
[19] T. Deng, H. Liu, Green Chem. 15 (2013) 116–124.
[20] Y. Kanie, K. Akiyama, M. Iwamoto, Catal. Today 178 (2011) 58–63.
[21] E.P. Maris, R.J. Davis, J. Catal. 249 (2007) 328–337.
[22] S. Wang, Y. Zhang, H. Liu, Chem. Asian J. 5 (2010) 1100–1111.
[23] A. Onda, T. Komatsu, T. Yashima, Phys. Chem. Chem. Phys. 2 (2000) 2999–3005.
[24] W.Q. Shen, G.A. Tompsett, R. Xing, W.C. Conner Jr., G.W. Huber, J. Catal. 286 (2012) 248–259.
[25] V.K. Díez, C.R. Apesteguía, J.I. Di Cosimo, J. Catal. 240 (2006) 235–244.
[26] M.A. Aramendía, V. Borau, C. Jiménez, A. Marinas, J. Marinas, J.R. Ruiz, F.J. Urbano, J. Mol. Catal. A 218 (2004) 81–90.
[27] R.M. Ravenelle, J.R. Copeland, W.G. Kim, J.C. Crittenden, C. Sievers, ACS Catal. 1 (2011) 552–561.